Acta of Bioengineering and Biomechanics
Vol. 20, No. 3, 2018

Original paper
DOI: 10.5277/ABB-01176-2018-02

Human cancellous bone mechanical properties and penetrator geometry in nanoindentation tests

ANNA M. MAKUCH*, KONSTANTY R. SKALSKI

Institute of Precision Mechanics, Departament of Mechanical Properties, Warsaw, Poland.

Purpose: The goal of the study was to determine the influence of the penetrator geometry on the human cancellous bone mechanical properties in indentation tests. The aim of this research was also the assessment of the material properties of bone structures, having in mind the energy aspects of the curve obtained in the cycle: inelastic loading and elastic unloading. *Methods*: The samples were resected from a femoral heads of patients qualified for a hip replacement surgery. During the Depth Sensing Indentation tests, hardness and elastic modulus of the cancellous bone tissue were measured using the spherical and Vickers penetrators. Measurements were made in a node and in a trabecula for each sample. *Results*: The analysis of the measurement results and the calculations of total energy, i.e., elastic and inelastic, and those of the parameters of hardness and elasticity made it possible to assess the influence of the penetrator geometry on the mechanical properties of bone structures at a microscopic level. *Conclusions*: It was found, with respect to the methodology of indentation, that without determining the shape of the penetrator and the site of the indentation, an objective assessment of the micro mechanical properties of the tested material is not possible.

Key words: *mechanical properties, indentation, cancellous bone, penetrator geometry, Young's modulus*

1. Introduction

One of the most important areas of research in biomechanics is associated with the use of experimental and numerical techniques in visualization and assessment of material and structural properties of tissues. Mechanical properties of a cancellous bone are heterogeneous at a level of microstructure (i.e., of trabeculae, osteons, and bone lamellae) [2], [11], and thus they can be assessed in a nanoindentation process by pushing a penetrator to the depth of a few microns in the tested medium forming the elastic half-space for a microscopic penetrator. Conducting these mentioned DSI (Depth Sensing Indentation) tests, e.g., on the osteons of the trabeculae of a cancellous bone, the elasticity and hardness of these bone tissues at a level of micro- and nanostructure can be determined.

When assessing the influence of the penetrator geometry on the mechanical properties of a cancellous bone in the study of nanoindentation, it is worth referring to the results of the works dedicated to nanoindentation in many aspects, including diversified structures (in particular porous), diversified materials (elastic, plastic, viscoelastic), strengthening of the material, a geometrically and materially diversified penetrator or numerical simulations supporting the experiment.

In the nanoindentation tests of tissues, the obtained results are influenced by many factors, such as: the degree of pathological changes, the state of tissue hydration, the anatomical location, the tested area, age, sex, process parameters and also limitations and assumptions of the method [9]. Among the sources of uncertainty and errors in the study of nanoindentation, not only of biological structures, J. Menčík [15] mentioned a number of features, such as: the properties of a penetrator, equipment, samples of the tested material, the initial penetration depth, temperature changes, the pile-up effect, the shape and the contact area in a penetrator–material configuration, the scale effect,

* Corresponding author: Anna Makuch, Institute of Precision Mechanics, Departament of Mechanical Properties, ul. Duchnicka 3, 01-796 Warsaw, Poland. Phone: +48225602946, e-mail: anna.makuch@imp.edu.pl

Received: July 23rd, 2018
Accepted for publication: October 18th, 2018

surface forces, the spread of the measured values and theoretical models used to assess the data.

The theoretical formulation of the issue of the influence of a penetrator on the deformation process in the study of indentation (the relation of force to the change of depth) was first formulated by Sneddon in his fundamental work of 1965 [21]. He presented it in the general solution to the Boussinesqu problem, i.e., pushing the penetrator into the elastic-plastic half-space, as well as the detailed solutions for some simple shapes of a penetrator (flat, cylindrical, conical, spherical, parabolic and ellipsoidal).

In the study of indentation, the resultative contact depth h_c and the contact area A_c resulting from the hollow h_c are not measured but they are determined on the basis of the analytical dependence of the total hollow of the penetrator h (sink-in model). However, when testing the materials with low hardness (with high E/Y) using the penetrator with a sharp tip, e.g., of Vickers or Berkovich, a different phenomenon (pile-up) occurs – the contact area is greater at the same load. Consequently, the calculative material stiffness is greater than in reality [15]. The error in the calculated value of A_c and, thus, the hardness maybe, according to Oliver and Pharr, even 60% [17].

The problem of the pile-up effect was undertaken in the works dedicated to numerical simulations of the indentation process carried out with the use of the spherical penetrator, usually with respect to the elastic-plastic materials [18], in particular metals [7], [25], more rarely to bones [4]. In Hernot's work [13], the dependence of the mechanical properties and the penetration depth on the radius of the spherical penetrator was studied. The numerical results of the simulation of testing the process of pushing the penetrator in the elastic-plastic half-space showed that the dependence between R and h can be described using the energy principle as a function of the reduced Young modulus E_R, the strengthening exponent n and the yield point of the material Re. In the work by M. Demiral et al. [4], the effects of anisotropy in a cortical bone were also studied numerically using a numerical model of the indentation with the use of a spherical penetrator. The parameters of elasticity and hardness in the axial direction and the transverse direction were determined.

The summary of the simulation results for the three types of a penetrator (of Berkovich, of Vickers and spherical one) in the indentation tests can be found in the work by N.A. Sakharov, J.V. Fernandes, J.M. Antunes, M.C. Oliveira [20]. Unlike spherical penetrators, pyramidal penetrators (of Vickers, of Berkovich) are often used not only in theoretical models [1], [14], but especially in experimental studies of various materials, such as: metals [23], ceramics [6], soda-lime glass, single crystals of aluminium, tungsten, and quartz [17]. Viscoelastic materials, such as plastics [16] and polymer composites as well as biological preparations are also experimentally studied. The aim of these mentioned works, was most frequently, to determine hardness and elasticity in the context of the conditions of force and velocity of loading/unloading, and hold time. The dependence of hardness and elasticity parameters is particularly evident in the case of materials with rheological properties [19]. In the study of composite materials with complex internal structure, the applied loading and indentation depth will significantly influence the resulting material properties (hardness, elasticity). In the work by J.M. Antunes, L.F. Menezes, J.V. Fernandes [1], the analysis for the Vickers penetrator was conducted paying special attention to the influence of geometrical inaccuracy of the tip on the results (hardness H_{IT} and elasticity E_{IT}) in the indentation tests. Making this mentioned assessment, it should be taken into account that the shape of the actual penetrator, i.e., the one used in the experiment, is not exemplary. Five values of the discrepancies of theoretical and actual profiles in materials with different mechanical properties were also tested, of hardness and elasticity in particular. The comparison of the experimental and numerical curves of loading/unloading shows the high correlation and the independence on the coefficient of friction. However, the experimental curves of unloading are characterized by a more intensive elastic reaction of the material, due to the very large but finite stiffness of the actual diamond penetrator. In the MES numerical calculations, it was noted that the concentration of stress in the area of the penetrator contact with the tested surface can lead to significant inaccuracies in the predicted hardness and elasticity.

In the indentation tests on biological preparations, the mechanical properties are most frequently determined for animal tissues (of an ox, a monkey, a pig, a rat) anatomically similar to a human tissue.

In this work [18], the spherical penetrator and the Berkovich penetrator were used in the tests of the long bones of a mouse. The results obtained suggest that the geometry of the penetrator, inter alia, influenced significantly the measured mechanical properties. These tests were carried out on a small tested sample (9 indentations in 2 wet and 2 dry samples – 36 indentations from a single animal in total). The authors obtained an average value of the module defined in the plane strain modulus for the Berkovich penetrator 20.1 ± 3.9 GPa (dry epoxy), 11.5 ± 2.0 GPa (wet epoxy) and for the

spherical penetrator (55 μm) 11.6 ± 1.7 GPa (dry epoxy), 9.2 ± 2.4 GPa (wet epoxy) using the analytical approach of Oliver–Pharr [17].

The assessment of the mechanical properties as a function of various indentation process parameters (force, hold time and velocity of loading/unloading) while using the Berkovich penetrator can be found in the work by J. Zhang, L. Niebur, T. Ovaert. The tests were carried out on animal preparations (of a monkey, of a bovine bone) stored in ethanol. The results obtained were compared to the results of numerical simulations. A similar comprehensive experimental study of the influence of test parameters on the mechanical properties of the trabecular structures of a human femoral head is shown in the work [13], in which the process energy parameters were also determined and the problem of a response of the material to deformation or potential strengthening of a tissue was discussed.

Z. Wu et al. [24] studied the effects of creep by using different hold time at constant force of loading/unloading (P_{max} = 10 mN), and constant velocity (v = 2 mN/sec) in the process of pushing the Berkovich penetrator in the sample cut from a femoral bone of an ox. The indentations were made in the area between the Haversian canal and the osteon edge of thecortical structure. Three rheological models of bone viscoelastic behaviour were considered: according to the linear model, the two-parameter Burgers model and the Kelvin model (linear solid, Burgers model, two-dashpot Kelvin model).

The influence of the distance between the successive indentations and the distance between the indentation and the pore in the indentation tests with the use of the Vickers penetrator and the Knoop penetrator was analysed in the work by W.M. Johnson and A.J. Rapoff [10]. The other factors were also analysed, such as: drying time, loading size, degree of hydration. The tests were carried out on monkey teeth and femoral bones of an ox.

The influence of temperature on the mechanical properties of a tissue was also tested on a bovine cortical bone in the strength tests (compression) and the nanoindentation tests. At a level of microstructure, the parameters of hardness and elasticity were determined using the Berkovich penetrator [12].

In the work by Isaksson et al. [8], the results of the indentation study for a cortical tissue and a trabecular tissue of a knee joint of an ox were presented (n = 8). The tests were carried out with a diamond penetrator in the shape of a cube (a cube corner diamond tip). The assessment of the influence of loading/unloading velocity on hardness and elasticity parameters and on dissipation energy was made, and also the semi-dynamic tests were carried out. The Burgers model was used to describe the viscoelastic features. The above-mentioned tests carried out on animal preparations are loaded with uncertainty stemming from the diversity of species, but, on the other hand, their advantage is the state of tissues (normal, unencumbered with any pathological changes).

In the case of still very few works dedicated to the study of human tissues, material resected during orthopaedic surgeries or coming from a corpse is most commonly used. E. Dall'Ara et al. [3] examined the samples of a trabecular bone (cut with a diamond saw) from 20 heads of human femoral bones without any lesions and 20 ones with diagnosed osteoarthritis. As a result of the nanoindentation tests with the use of the Vickers penetrator, it was found that the hardness (Hv) of the tissues affected by arthrosis is by about 13% lower than that of normal tissues. In the case of arthrosis, the probability of finding the lamellae of the secondary osteons (SO) is higher than in the case of the structures, which are not pathologically changed. The parallel-lamellae (PL) are harder by about 10% than the secondary osteons both in the case of arthrosis and of normal tissues. The recorded average hardness of PL and SO was respectively (34.1 H_V and 30.8 H_V) for the normal structures and for the structures affected by the disease it was (30.2 H_V and 27.1 H_V). These obtained results do not allow settling if the trabecular bone hardness depends on sex or age. The authors of this work point to the need for further studies on a larger sample group.

Human tissues with osteoarthritis (the number of the samples n = 9) were also the subject of the analysis in the work [22]. The authors formulated the conclusions concerning the source of changes in the structure of bones in the diseases of joints (Osteoarthritis – OA) based on the: indentation tests (measurement of hardness and elasticity with the Vickers penetrator), Raman spectroscopy (check of the degree of bone mineralization), micro computed tomography μCT (assessment of the changes in bone density). In the tests of nanoindentation on average, the following results were obtained: 44–53 H_V and 8.7–11.8 GPa for the state I OA, 41–43 H_V and 7–8.3 GPa for the state II OA and 39–45 H_V and 8.6–10.7 GPa for the state III OA.

The viscoelastic properties of the human cortical tissue (the core of the tibia) without lesions were tested by the nanoindentation method using the Berkovich penetrator by Z. Fan and J.Y. Rho [5]. The mechanical properties were measured by two techniques: by the quasi-static one, in which theresponse of the material to different velocities of the incremental load-

ing/unloading (10–1000 μN/s) is estimated, while the velocity of deformation is kept constant; and by the dynamic technique (with the set frequency/frequency-specific dynamic technique), in which the response of the material to different loads changing at a constant rate with the fixed (180 s) or variable hold time (10–1000 s) is assessed. It was observed that the registered modulus of elasticity E was exponentially dependent on the velocity of deformation and the value of the designated exponent (d = 0.06) was within the range of the results obtained in conventional tests (d = 0.057–0.61).

The aim of this work was to assess the influence of the geometry of the two types of a penetrator (spherical and Vickers) on the mechanical properties of a trabecular human bone (in nodes and in trabeculae) in nanoindentation tests. In particular, energy aspects of the process of loading/unloading were examined. The possible implications resulting from the applied method of mathematical description of the penetrator geometry and the differences between the theoretical model and the actual object were indicated. The work also takes into consideration clinical aspects, including an attempt to answer the question of how the factors, such as the type of disease (arthritis, osteoporotic fractures), age and sex of patients, influence the mechanical properties of a bone tissue being tested at the level of microstructure. This type of comprehensive study and analyses carried out with the use various penetrators on human preparations will complement the existing knowledge within the range of mechanical properties of bone structures at a level of microstructure.

2. Materials and methods

2.1. Models of penetrators and their contact area

The analytical solution for an elastic contact when pressing an axially symmetric penetrator in the half-space was presented by Sneddon in his fundamental work [21], based on the earlier approach of Boussinesqu. As a result, he obtained simple relations: loading force (P) – the depth of penetration (h) for a wide variety of penetrator shapes – flat, spherical, conical; these relations are expressed in the form of a power law:

$$P(h) = CEh^n \tag{1}$$

wherein: E – modulus of elasticity; C – dimensionless coefficient; n – strain-hardening coefficient

Geometric models and their characteristic values are shown in Fig. 1, according to the interpretation by Sakai [19]. The important parameter in the description of the mechanics of contact is the mentioned depth related to the area of direct contact (projection) A_c, which express respectively for each penetrator: flat (f), spherical (s) and conical (c):

$$A_{c,f} = \frac{\pi d^2}{4}, \quad A_{c,s} = \pi r^2,$$
$$A_{c,c} = \pi r^2 = g h_c^2 = \pi \operatorname{ctg}^2 \beta h_c^2 \tag{2}$$

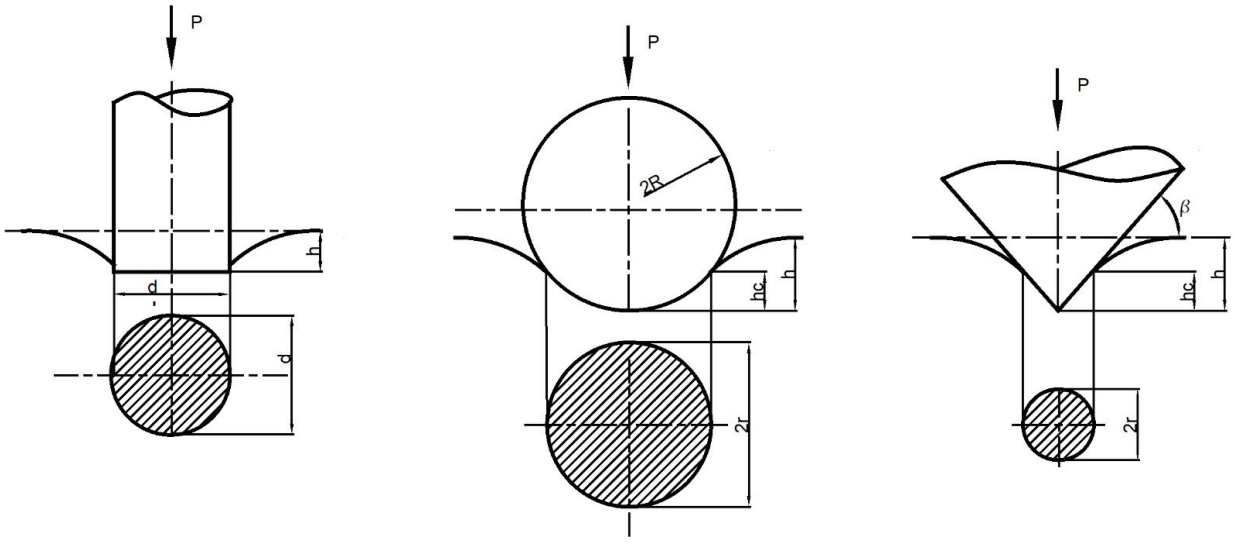

Fig. 1. Diagram of pressing the penetrator: flat (a), spherical (b), conical (c) in the elastic half-space by P force, where the penetrator geometry (β, R), penetration depth (h) and the appropriate dimensions of the contact area projection (d, r) are marked

An important relation, as shown in Fig. 1, is also a linear correlation of the penetration depth of the penetrator (h) and the contact depth (h_c), i.e.,

$$h = \gamma h_c \tag{3}$$

wherein: the coefficient takes values $\gamma_f = 1$; $\gamma_s = 2$; $\gamma_c = \pi/2$; for a flat penetrator, a spherical one, a conical one, respectively.

Characterization of geometry and material described by the coefficient C for the flat, spherical and conical models is expressed respectively as follows:

$$C_f = \frac{d}{1-\nu^2} \quad C_s = \frac{4R}{3(1-\nu^2)}\left(\frac{2}{\frac{h}{h_c}}\right)^{3/2}$$

$$C_c = \frac{\operatorname{tg}\beta}{2(1-\nu^2)}\frac{\pi \operatorname{ctg}^2\beta}{\left(\frac{h}{h_c}\right)^2} \tag{4}$$

where in: ν – Poisson's ratio.

The reflections on an analytical solution of an elastic contact of an axially symmetric penetrator can easily be used to formulate the constitutive equation. Thus, for the conversion from the force-penetration depth space (P–h) in the space of the averaged values of the stresses-deformations, the postulated relations may be used:

$$\overline{\sigma} = \frac{P}{\frac{\pi d^2}{4}} \quad \overline{\sigma} = \frac{P}{\pi r^2} = \gamma_s \frac{P}{2\pi R h}$$

$$\overline{\sigma} = \frac{P}{\pi r^2} = \gamma_c^2 \frac{P}{g h^2} \tag{5}$$

and respectively for the averaged deformations $\overline{\varepsilon}$ (in the incremental form $d\overline{\varepsilon}$):

$$d\overline{\varepsilon} = K_f \frac{dh}{d} \quad d\overline{\varepsilon} = K_s \frac{dr}{R} \quad d\overline{\varepsilon} = K_c \frac{dh}{h} \tag{6}$$

wherein the coefficients K, depending on the geometry of the penetrator, are as follows:

$$K_f = K_s = \frac{4}{\pi} \qquad K_c = \operatorname{tg}\beta \tag{7}$$

The constitutive equation for the deformed elastic center can be approximated by the following relation:

$$d\overline{\sigma} = \frac{E}{1-\nu^2} d\overline{\varepsilon} \tag{8}$$

These analytical considerations show how the behavior of the material described by constitutive equations (including stress, strain) depends on the shape of the penetrator, in particular with respect to the shapes of penetrators having the greatest importance in practice. The cases of spherical and Vickers are of interest for practical applications.

In the nanoindentation analysis, force and total work in the loading process can be described by the relations introducing scaling functions Π(.) [25]:

$$P = Eh^2 \Pi_\alpha\left(\frac{\sigma_Y}{E}, \nu, n, \theta\right) \tag{9}$$

$$W_{\text{tot}} = \int_0^{h_m} P dh = \frac{Eh_m^3}{3}\Pi_L\left(\frac{\sigma_Y}{E}, \nu, n, \theta\right) \tag{10}$$

wherein: in this case $\Pi_L\left(\frac{\sigma_Y}{E}, \nu, n, \theta\right)$ – the dimensionless scaling function depends on four parameters, θ – the half angle of the penetrator, and σ_Y – a limit value of the stresses for elastic deformations.

However, in the process of unloading work (Fig. 2) will be as follows:

$$W_u = \int_{h_f}^{h_m} P dh = Eh_m^3 \Pi_u\left(\frac{\sigma_Y}{E}, \frac{h_f}{h_m}, \nu, n, \theta\right) \tag{11}$$

wherein Π_u – the dimensionless scaling function depends on five parameters.

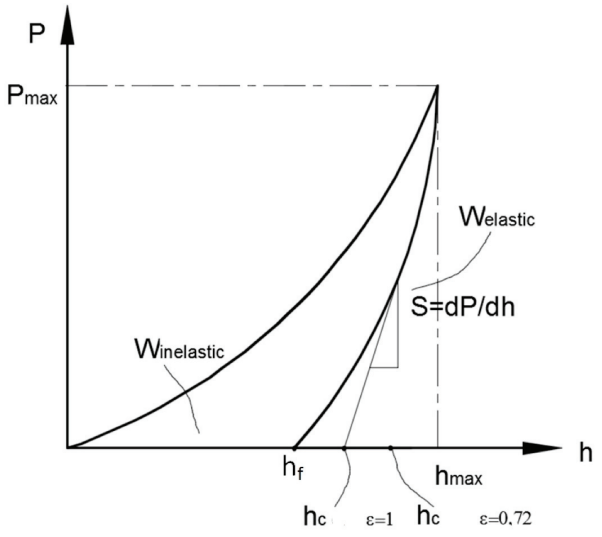

Fig. 2. The curve of loading/unloading recorded in the indentation process

The relative ratio of irreversible work to total work in the indentation process can thus be written down as follows:

$$\frac{W_{\text{tot}}-W_u}{W_{\text{tot}}}=1-3\frac{\Pi_u\left(\frac{\sigma_Y}{E},\frac{h_f}{h_m},v,n,\theta\right)}{\Pi_L\left(\frac{\sigma_Y}{E},v,n,\theta\right)}$$

$$=\Pi_W\left(\frac{\sigma_Y}{E},\frac{h_f}{h_m},v,n,\theta\right) \tag{12}$$

This ratio is dependent, inter alia, on the final h_j and the maximum depth of unloading h_m.

The results of numerical simulations carried out for the materials with different strain-hardening index (n = 0.0–0.5), and Poisson's ratio (v = 0.2–0.4) indicates linear relation between H/E (hardness/elasticity), and the value of $\frac{W_{\text{tot}}-W_u}{W_{\text{tot}}}$, which can be written down with the following proportional relation:

$$\frac{H}{E^*}\approx\frac{W_{\text{tot}}-W_u}{W_{\text{tot}}} \tag{13}$$

The relative unloading work in the process of indentation expressed in (12) and (13) is interesting because of the significant correlation with the values measured by this method, and which include, inter alia, E_{IT} elasticity modulus and H_{IT} material hardness [13]. These relations can be written down as follows:

$$\frac{W_{\text{tot}}-W_u}{W_{\text{tot}}}=1-k\frac{\Pi_u\left(\frac{\sigma_Y}{E},\frac{h_f}{h_m},v,n,\theta\right)}{\Pi_L\left(\frac{\sigma_Y}{E},v,n,\theta\right)}=1-k\frac{H_{IT}}{E_{IT}} \tag{14}$$

$$1-\frac{W_u}{W_{tot}}=1-k\frac{H_{IT}}{E_{IT}} \tag{15}$$

$$\frac{W_u}{W_{\text{tot}}}=k\frac{H_{IT}}{E_{IT}}\Rightarrow\frac{W_u}{W_{\text{tot}}}\sim\frac{H_{IT}}{E_{IT}} \tag{16}$$

wherein: k – expresses the coefficient of geometry and material interpreting the ability of the center to deform (potentially to strengthen) [17].

2.2. Material for studies

Cancellous bone tissues were used as the experimental material. A patient qualified for a hip replacement surgery had his femoral head routinely resected. With the approval of the Bioethics Committee of the Military Medical Institute, the resected elements were taken and stored in the database of preparations. After the preparation of the samples with the dimensions of 20 × 20 × 20 mm from these elements, they were used for the studies of biomechanical properties of bone tissues, taking the development of the classification method into account.

There are many factors that have a significant influence on bone mineralization, which results in mechanical properties of hard tissues. Among them, inter alia, ages, sex, genetics, the medications taken, including anticoagulants, antibiotics or steroids, are mentioned. On the other hand, it is assumed that certain parameters of histopathology (the number of osteocytes, gaps between trabeculae, and the dimensions of trabeculae) will translate into specified material properties. For example, in the case of fractures resulting from the osteoporotic changes, the number of osteocytes is smaller.

So, the main division of the experimental group (preparations), from a clinical point of view, included fractures resulting from the osteoporotic changes, and degenerative changes in a hip joint (arthrosis). In the case of fractures resulting from the osteoporotic changes, to make an assessment and qualifications for arthroplasty the following scales, which indicate the degree of proximal displacement are used: Pauwels's (degrees II/III – are qualified for arthroplasty), Linton's (degrees II/III), Garden's (IV) SOEUR (type I), Watson-Jones's (type III). In contrast, degenerative changes in a hip joint (arthrosis), which are qualified for arthroplasty, are characterized by a narrowing of a joint gap, osteophytes, cysts, pain, limited efficiency, dysfunctions assessed on Kellgren–Lawrence's scale (degrees III/IV are qualified for arthroplasty) Altman's (degrees II/III), IRF – Individual Radiographic Feature) (degree III).

Taking the criteria of age, sex and clinical diagnosis into account, 8 following groups were selected in the studies: I. Fractures – women over 50 years of age; II. Fractures – women under 50 years of age; III. Fractures – men over 50 years of age; IV. Fractures – men under 50 years of age; V. Arthrosis – women over 60 years of age; VI. Arthrosis – women under 60 years of age; VII. Arthrosis – men above 60 years of age; VIII. Arthrosis – men under 60 years of age.

To study the influence of the penetrator shape on the selected mechanical properties of the bone tissue, 7 samples cut from 7 femoral heads (of the patients undergoing a knee replacement surgery between the ages of 48 to 76) were selected, including 3 samples in which osteoporotic changes were stated and 4 samples with degenerative changes. In the population, five samples came from men and two from women. On each sample, 7 measurements were taken in the trabeculae (B) and 7 in the nodes (N).

The following designations of the samples were adopted: 1 (woman, 62 years old, arthrosis), 2 (man, 71 years old, arthrosis), 3 (man, 68 years old, arthrosis), 4 (woman, 69 years old, osteoporotic fracture), 5 (man, 76 years old, arthrosis), 6 (man, 52 years old, osteoporotic fracture), 7 (man, 48 years old, osteoporotic fracture).

2.3. Test stand

The study of mechanical properties and in particular of the influence of the penetrator shape used in nanoindentation tests on the mechanical properties of a cancellous bone (hardness, elasticity, work) performed in the nodes and in the trabeculae were carried out on the CSM Microhardness Tester whose schematic diagram is illustrated in Fig. 3.

by means of a microscope in such way as to make it free from defects and locate it centrally as far as possible from the pores. The study of the influence of the distance from the pores on the measured values of mechanical parameters, which was conducted by Johnson [10] showed that making the indentations in the place close to the Havers channels or to the pores results in gaining the results significantly affected by a measurement error. Thus, 7 measurements were taken in the trabecula and 7 in the node (in the place of a combination of several trabeculae) of each sample.

The evaluation of the indentation geometry and location in the nanoindentation test was carried out by means of the 2D optical microscope (NICON ECLIPSE LV150 coupled with the computer-assisted image analyser NIS-Elements BR 3.0) and the 3D optical microscope (Keyence VHX 5000).

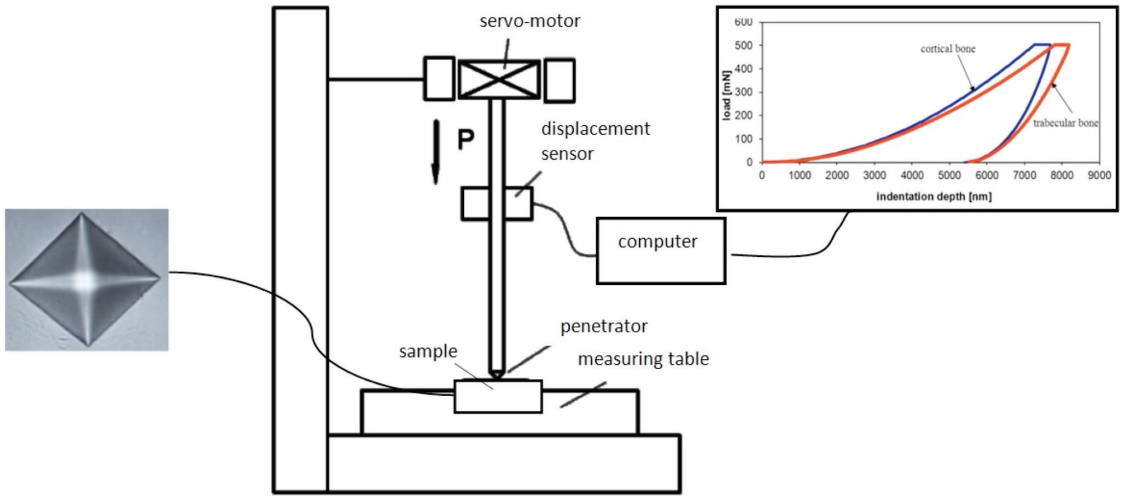

Fig. 3. Schematic diagram of the test stand for the measurement of the properties and bone material structures using the DSI method [28]

Two types of a penetrator were tested: Vickers (α = 136°) and spherical (∅ 200 μm). All the tests were conducted on the test stand using the same parameters: loading/unloading velocity v = 500 mN/min, force P_{max} = 500 mN and hold time τ = 20 s. The measurements were performed in a controlled environment (temperature of 20 ± 0.5 °C, air humidity 32 ± 5%). The samples were drained from the alcohol in an atmosphere of room temperature for one hour before starting the test (such a method of storing the preparations for indentation tests can also be found in the works of [8], [13].

The measurements were repeated several times in different places of the tissue sample. Before performing the indentation, the place of a hollow was chosen

3. Results

The structural studies of the samples of a cancellous bone undergoing the indentation test made it possible to assess the size and the geometry of the indentation after unloading, which is correlated with the actual contact area. Figure 4a indicates the exemplary dimensions characteristic for the indentation obtained from the Vickers penetrator (diagonal length) and the spherical penetrator (corresponding to the diameter of the sphere segment projection on the tested area). Figure 4b shows the regions of trabecular structure denoted by the trabecula B and the node N (point of the connection of several trabeculae).

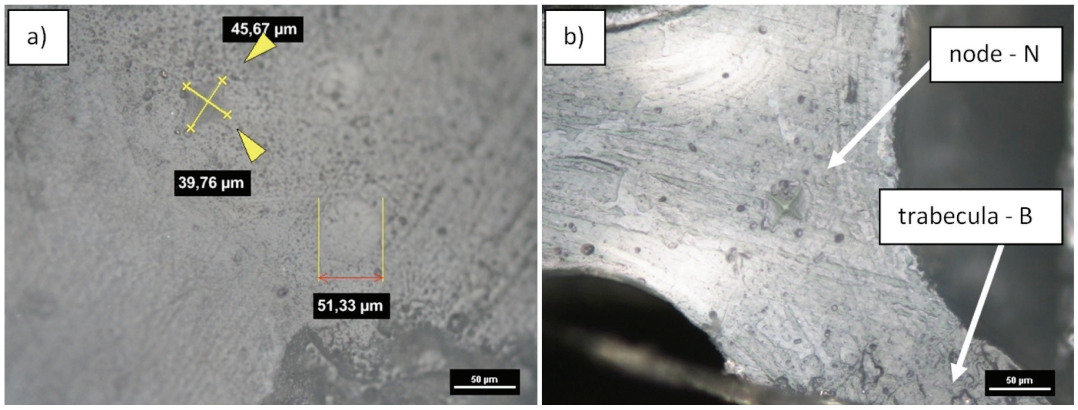

Fig. 4. Microscopic view of the bone trabecula in sample *2* with the exemplary characteristic dimensions of indentations (a) and the marked place of performing the measurement in the indentation test by means of the Vickers penetrator ($\alpha = 136°$) and the spherical penetrator (∅ 200 µm)

Figures 5–8 summarize the measurement results of the average values of indentation microhardness H_{IT} and elasticity E_{IT}. They concern the series of 7 measurements taken at different places of indentation in the node and in the trabecula by two types of penetrators (spherical and Vickers). This represents a total of 196 measurements.

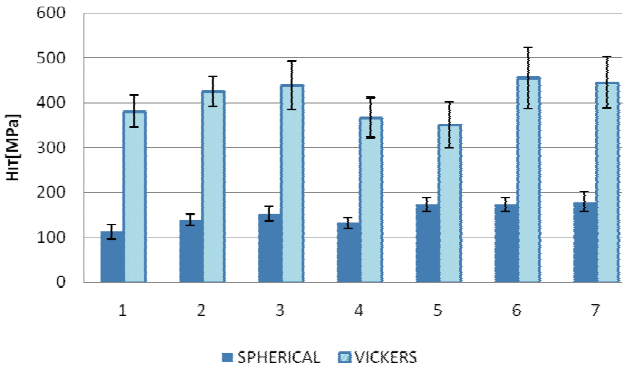

Fig. 5. Comparison of the average hardness values H_{IT} [MPa] for the trabecular bone; $\tau = 20$s, $P_{max} = 500$ mN in the node measured by the spherical penetrator (∅ 200 µm) and the Vickers penetrator ($\alpha = 136°$)

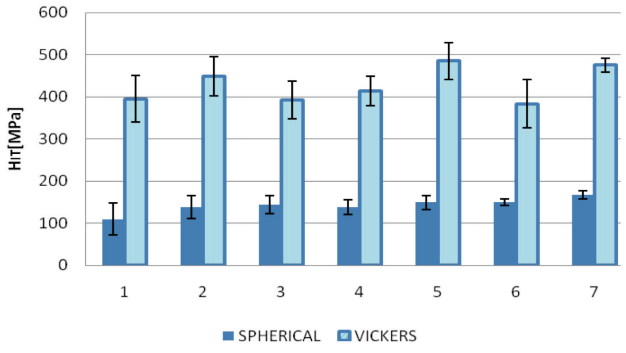

Fig. 6. Comparison of the average hardness values H_{IT} for the trabecular bone; $\tau = 20$ s, $P_{max} = 500$ mN in the trabecula measured by the spherical penetrator (∅ 200 µm) and the Vickers penetrator ($\alpha = 136°$)

The indentation hardness values (H_{IT}) measured for the Vickers penetrator occurred to be much higher (even 3 times) than for the spherical penetrator, which is clearly shown in the graphs (Figs. 5 and 6).

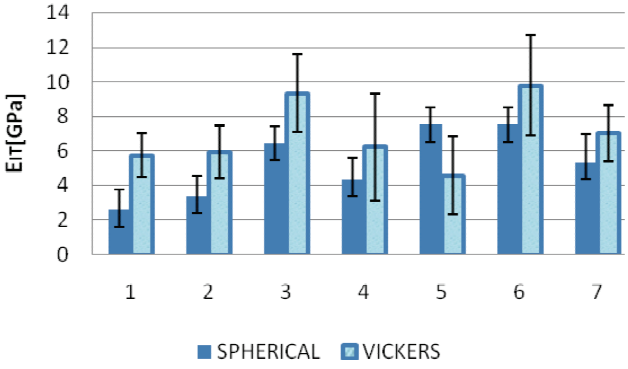

Fig. 7. Comparison of the average values of the elastic modulus E_{IT} for a trabecular bone; $\tau = 20$ s, $P_{max} = 500$ mN in the node measured with the use of the spherical penetrator (∅ 200 µm) and the Vickers i penetrator($\alpha = 136°$)

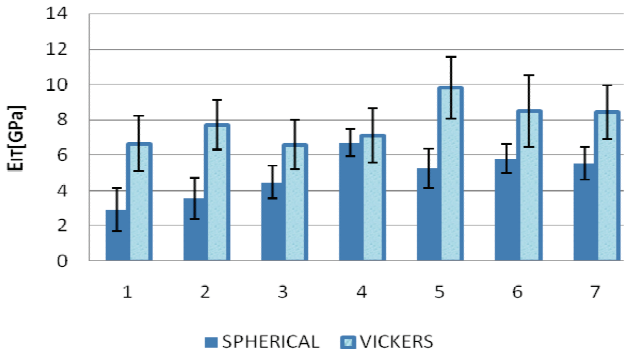

Fig. 8. Comparison of the average values of the elastic modulus E_{IT} for a trabecular bone; $\tau = 20$ s, $P_{max} = 500$ mN in the trabecula measured with the use of the spherical penetrator (∅ 200 µm) and the Vickers penetrator ($\alpha = 136°$)

Analogically to the studies on hardness, the influence of the penetrator shape on the elastic properties

of the tissues in the node and in the trabecula was also evaluated (Young's modulus E_{IT} was used as measurement). Bar graphs in Figs. 7 and 8 highlight the significant differences in the values for both penetrators: spherical (∅ 200 μm) and Vickers (α = 136°). It is also possible to notice a greater spread of the measured values in the case of the spherical penetrator test.

Comparing the charts in Figs. 5 and 6 to the charts in Figs. 7 and 8, it is not possible to observe any significant differences in the parameters of hardness and elasticity for the area of the trabecula and the node. In order to determine the bone tissue ability to accumulate the total energy (inelastic work) of material deformation, the area under the loading/unloading curve ($W_{\text{inelastic}}$) was determined by integration. The total energy W_{total} was also determined. The difference of these values is associated with an elastic response of the material to the process of penetration of the penetrator into the material, i.e., W_{elastic} [13].

Knowing the hardness and elasticity parameters as well as a relative measure of the deformation energy (determined by the difference between the total energy and the elastic energy) it is possible to estimate the constant k from the Eqs. (13) derived by M. Zhao et al. [25].

Table 1 presents the average values of energy parameters $W_{\text{inelastic}}$, W_{total}, W_{elastic} and k factor, measured in the node and in the trabecula of the cancellous bone structure. These measurements were taken by the spherical penetrator and the Vickers penetrator at constant velocity v = 500 mN/min (loading/unloading), constant hold time τ = 20 s and constant maximum loading force $P_{\max}$ = 500 mN.

It can be noticed that inelastic energy in the loading/unloading process performed by the Vickers penetrator is more than twice higher than in the test performed by the spherical penetrator; the difference is also detectable in the results between the measurements in the trabecula (B) and in the node (N). Similar relationships can be also seen in the values of the total work – W_{total}.

However, the elastic deformation work does not show any clear dependence on the type of a penetrator. In the case of the tests performed in the area of the trabecula, its values for the spherical penetrator and the Vickers penetrator are similar. A similar correlation can be observed for the tests performed in the node.

The coefficient of geometry and material k, which is analytically determined based on parameters of hardness and elasticity and of energy, is substantially greater for the spherical penetrator than for the Vickers penetrator; this concerns both the test in the node and in the trabecula.

In order to estimate the left-right-hand form of the Eq. (14), the additional graphs H_{IT}/E_{IT} and W_{total}–Wu/W_{total} (Figs. 9–12) were developed, separately for the measurements taken in the node and in the trabecula.

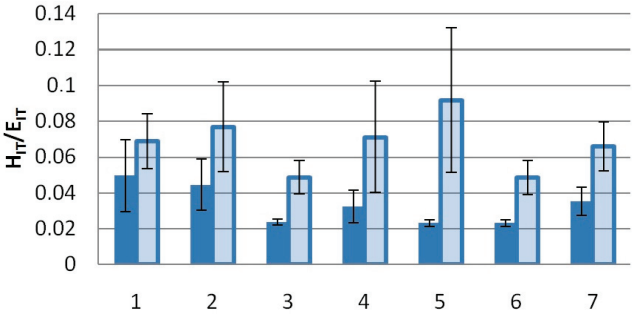

Fig. 9. The ratio of hardness to indentation elasticity measured in the node in the indentation test by the spherical penetrator and the Vickers penetrator

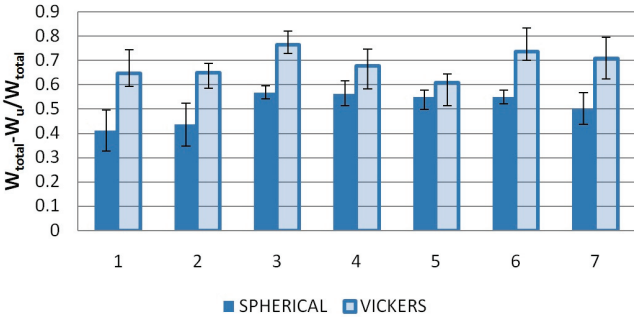

Fig. 10. The ratio of inelastic deformation work to total work measured in the node in the indentation test by the spherical penetrator and the Vickers penetrator

Table 1. Average values for the hysteresis fields of the loading/unloading curves and k coefficient for a trabecular bone tested in the node and in the trabecula by two types of penetrators

Parameter	Vickers (α = 136°)		Spherical (∅ 200 μm)	
	Trabecula	Node	Trabecula	Node
$W_{\text{inelastic}}$ [Nm]	$1.14\cdot10^{-6} \pm 7.51\cdot10^{-8}$	$1.16\cdot10^{-6} \pm 9.74\cdot10^{-8}$	$4.26\text{E}\cdot10^{-7} \pm 9.92\cdot10^{-8}$	$4.05\cdot10^{-7} \pm 7.11\text{E}\cdot10^{-8}$
W_{elastic} [Nm]	$4.75\cdot10^{-7} \pm 9.49\cdot10^{-8}$	$5.63\cdot10^{-7} \pm 2.57\cdot10^{-7}$	$4.40\cdot10^{-7} \pm 1.53\cdot10^{-7}$	$4.20\cdot10^{-7} \pm 2.21\text{E}\cdot10^{-7}$
W_{total} [Nm]	$1.61\cdot10^{-6} \pm 1.39\cdot10^{-7}$	$1.72\cdot10^{-6} \pm 2.94\cdot10^{-7}$	$8.66\cdot10^{-7} \pm 2.35\cdot10^{-7}$	$8.25\cdot10^{-7} \pm 2.66\cdot10^{-7}$
k [–]	5.22 ± 0.56	4.84 ± 0.67	16.31 ± 2.21	16.00 ± 3.47

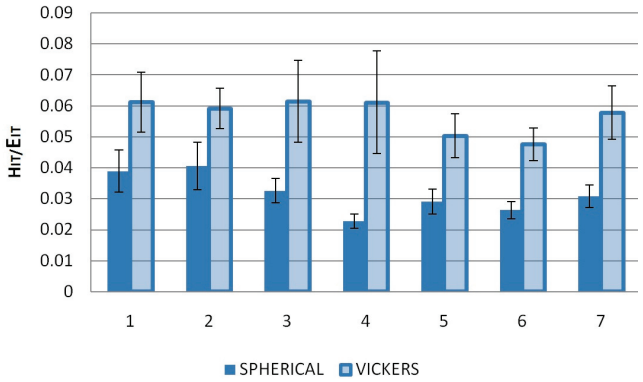

Fig. 11. The ratio of hardness to indentation elasticity measured in the trabecula in the indentation test by the spherical penetrator and the Vickers penetrator

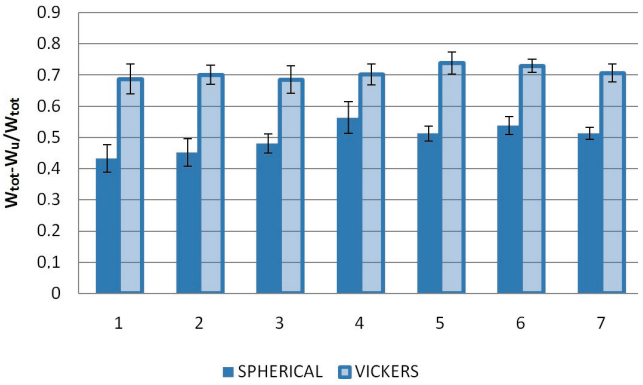

Fig. 12. The ratio of inelastic deformation work to total work measured in the trabecula in the indentation test by the spherical penetrator and the Vickers penetrator

Assuming, according to the Eq. (14), that the ratio of inelastic deformation work to total work in the indentation test (W_{total}–W_u/W_{total}) is a function of the ratio of hardness to indentation elasticity (H_{IT}/E_{IT}), it can be seen (Figs. 13–14) that there is a linear correlation between these values and that its measure is the coefficient k.

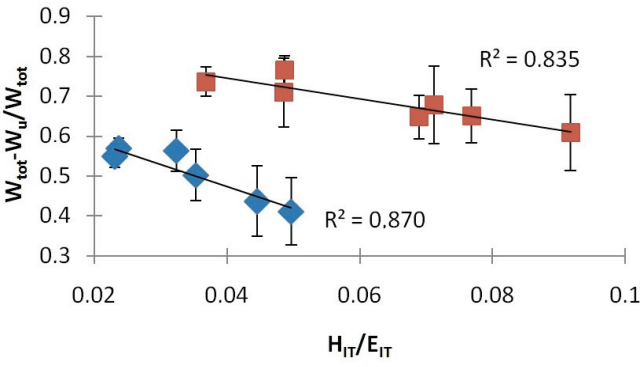

Fig. 13. The ratio of inelastic deformation work to total work in the indentation test as a function of the ratio of hardness to elasticity in the indentation test performed in the node

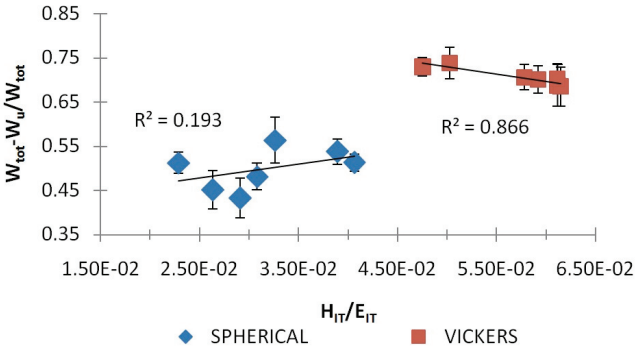

Fig. 14. The ratio of inelastic deformation work to total work in the indentation test as a function of the ratio of hardness to elasticity in the indentation test performed in the trabecula

4. Discussion

In order to better understand the influence of the penetrator geometry on the behaviour of the material in the indentation process, the comparative indentation tests using the spherical penetrator (Ø 200 μm) and the Vickers penetrator (α = 136°) were performed. These tests were carried out on the samples of a cancellous bone derived from of a human femoral head.

Based on the above-mentioned studies, the following conclusions can be made.

With confidence it can be stated that the penetrator geometry had the significant influence on the measured mechanical properties of bone tissues. The parameters of hardness (H_{IT}), obtained in the indentation test by means of the spherical penetrator are about 3 times smaller than the parameters measured for the Vickers penetrator. In contrast, the elasticity modulus (E_{IT}) for the spherical penetrator is from 7% to even more than 50% smaller than for the Vickers penetrator. And the spread of values is greater in the case of the test done using the spherical penetrator. This is consistent with the observations of N. Rodriguez-Florez et al. [30], who, in relation to the long bones of mice, noted that the shape of the penetrator (spherical/Berkovich) largely implies the range of the parameters characterizing the mechanical properties obtained in the indentation test. Moreover, in the said test the recorded value of the elastic modulus was smaller by approx. 25% for the spherical penetrator than for the Berkovich penetrator in the case a wet tissue. The difference became even more clearly apparent in the case of a dry tissue (up to 73%).

The values of H_{IT} and E_{IT} obtained for the measurement done using the sharp type penetrator are consistent with, inter alia, the values obtained by other

research teams in nanoindentation tests of a trabecular tissue [13], [22]. The values obtained by measuring using the spherical penetrator can be compared mainly with the results obtained in the numerical simulations [4]. However, due to the use of different methods, such statement does not give an adequate picture of the observed changes. For this particular case of a trabecular bone, a more accurate numerical model with additional boundary conditions should be developed rather than the one presented in [4].

The inelastic energy (and consequently also the total energy) in the process of loading/unloading of bony structures carried out with the use of the spherical penetrator is more than twice smaller than in the case of the tests performed with the use of the Vickers penetrator. Because the test parameters (velocity and loading/unloading force, hold time) were the same, the difference in the results should be sought in a different depth of contact indentation and in a different contact area.

Analyzing the obtained results, it cannot be stated that the bone in the node is clearly weaker/stronger than in the trabecula, although the differences were expected because of different orientation of lamellae in trabeculae (a stock of parallel lamellae is perpendicular to the direction of performing the indentation) and in the nodes (lamellae arranged concentrically and their axis coincides with the test direction). There are no comparative studies in this regard. Such dependences are not stated for both the spherical penetrator and the Vickers penetrator.

In the case of the use of the sharp type penetrator, it can be noticed that the material response to deformation in the form of total, elastic and inelastic work was greater in the test of the structure in the node than in the test in the trabecula. This was accompanied by a slight decline in the value of the coefficient k.

During the tests performed by the spherical penetrator, the inverse material response was observed, i.e., greater total work (elastic and inelastic) was made in the area of the trabecula, and the designated coefficient k was higher than when it is measured in the node under unchanged conditions of the indentation test.

In the tests performed, the penetrator occurred to sink into the trabecula to a depth of 4 to 11 μm when the thickness of a single bone lamina (lamella) was 2–4 μm.

For the tests performed in the node, the penetrator moved in the axis close to the perpendicular to the plane of the osteon section. As a result, the elastic and inelastic deformation (plastic–viscoelastic) occurred in an axial direction of a single bone lamella. This lamella was created by spring (arranged spirally) collagen fibers reinforced by hydroxyapatite.

When the test was conducted in the area of the trabecula, the compression and durable deformation of several bone lamellae occurred (probably) and they acted as a layer composite. This could explain the growth of the energy values in the test performed by the spherical penetrator in the trabecula, in contrast to the test in the node, in which probably more elastic deformation and energy dissipation occurred due to the viscoelastic properties of the material.

The tests performed show a clear correlation between a patient's age and the hardness and elasticity of a bone. As expected, the higher parameters of E_{IT} and H_{IT} were recorded in the case of younger patients. However, based on the tests performed, it is not possible to formulate any clear conclusions on the influence of the nature of pathological changes (osteoporotic fractures and degenerative changes were considered) on the mechanical properties of bone structures at a level of microstructure. The full assessment, with taking the material and histopathological properties of a human cancellous bone tissue into account, should be subjected to further studies.

5. Conclusions

The main conclusion is that the penetrator geometry had the significant influence on the measured mechanical properties of bone tissues. Summing up, it can be stated that the implications arising from the adapted method of a mathematical description of the penetrator geometry and the differences between the theoretical model and the real object, in the case of the studies on bone structures (and not only), have a deep physical meaning, which is evidenced by the conducted experimental studies. The comprehensive tests and the analysis carried out on human preparations, using various penetrators, can supplement the existing knowledge in the field of mechanical properties of bone structures at the level of the microstructure and the factors affecting them. In particular, it will contribute to a better understanding of the mechanisms of the deformation of cancellous bone tissues (of lamellae, osteons) which undergo overloading. The shape of the penetrator significantly influences the received values and the accuracy of the measurements.

Acknowledgement

The study was financed by the National Science Centre of Poland – project No. 2014/15/B/ST7/03244.

References

[1] ANTUNES J.M., MENEZES L.F., FERNANDES J.V., *Influence of Vickers tip imperfection on depth sensing indentation tests*, Int. J. Solids Struct., 2007, 44, 2732–2747.

[2] COUTTS L.V., JENKINS T., LI T., DUNLOP D.G., OREFFO R.O., COOPER C., HARVEY N.C., THURNER P.J., *Variability in reference point microindentation and recommendations for testing cortical bone: Location, thickness and orientation heterogeneity*, J. Mech. Behav. Biomed. Mater., 2015, 46, 292–304.

[3] DALL'ARA E., ÖHMAN C., BALEANI M., VICECONTI M., *Reduced tissue hardness of trabecular bone is associated with severe osteoarthritis*, J. Biomech., 2011, 44, 1593–1598.

[4] DEMIRAL M., ABDEL-WAHAB A., SILBERSCHMIDT V., *A numerical study on indentation properties of cortical bone tissue: Influence of anisotropy*, Acta Bioeng. Biomech., 2015, 17(2), 3–14.

[5] FAN Z., RHO J.Y., *Effects of viscoelasticity and time-dependent plasticity on nanoindentation measurements of human cortical bone*, J. Biomed. Mater. Res. A, 2003, 67(1), 208–214.

[6] GUBICZA J., JUHASZ A., TASNADI P., ARATO P., VOROS G., *Determination of the hardness and elastic modulus from continuous Vickers*, J. Mater. Sci., 1996, 31, 3109–3114.

[7] HAUŠILD P., NOHAVA J., MATERNA A., *Identification of stress-strain relation of austenitic steels by instrumented indentation*, Chem. Letters, 2011, 105, 676–679.

[8] ISAKSSON H., NAGAO S., MAŁKIEWICZ M., JULKUNEN P., SMITH R., JURVELIN J.S., *Precision of nanoindentation protocols for measurement of viscoelasticity in cortical and trabecular bone*, J. Biomech., 2010, 43, 2410–2417.

[9] JIROUŠEK O., *Nanoindentation of Human trabecular bone – Tissue Mechanical Properties Compared to Standard Test Methods Engineering*, Nanoindentation in Materials Science, 2012.

[10] JOHNSON W.M., RAPOFF A.J., *Microindentation in bone: Hardness variation with five independent variables*, J. Mater. Sci. – Mater. M., 2007, 18, 591–597.

[11] KATSAMENIS O.L., JENKINS T., THURNER P.J., *Toughness and damage susceptibility in human cortical bone is proportional to mechanical in homogeneity at the osteonal-level*, Bone, 2015, 76, 158–168.

[12] LAU M.L., LAU K.T., KU H., BAHATTACHARYYA D., YAO Y.D., *Measurements of Heat Treatment Effects on Bovine Cortical Bones by Nanoindentation and Compression*, J. Biomat. Nanobiotech., 2012, 3, 105–113.

[13] MAKUCH A., SKALSKI K., PAWLIKOWSKI M., *The influence of the cumulated deformation energy in the measurement by the DSI method on the selected mechanical properties of bone tissues*, Acta Bioeng. Biomech., 2017, 19(2), 79–91.

[14] MAZERAN P.E., BEYAOUI M., BIGERELLE M., GUIGON M., *Determination of mechanical properties by nanoindentation in the case of viscous materials*, Int. J. Mat. Res., 2012, 103(6), 715–721.

[15] MENČÍK J., *Uncertainties and Errors in Nanoindentation, Nanoindentation in Materials Science*, InTech, Jiri Nemecek (ed.), 2012.

[16] OLIVEIRA G.L., COSTA C.A., TEIXEIRA S.C.S., COSTA M.F., *The use of nano- and micro-instrumented indentation tests to evaluate viscoelastic behavior of poly (vinylidene fluoride) (PVDF)*, Polym. Test., 2014, 34, 10–16.

[17] OLIVIER W.C., PHARR G.M., *An improved technique for Determining hardness and elastic modulus-using load and displacement sensing indentation experiments*, J. Mater. Res., 1992, 7(6), 1564–1583.

[18] RODRIGUEZ-FLOREZ N., OYEN M.L., SHEFELBINE S.J., *Insight into differences in nanoindentation properties of bone*, J. Mech. Behav. Biomed. Mater., 2013, 18, 90–99.

[19] SAKAI M., *Time-dependent viscoelastic relation between load and penetration for an axisymmetric Indenter*, Philos. Mag. A, 2002, 82(10), 1841–1849.

[20] SAKHAROV N.A., FERNANDES J.V., ANTUNES J.M., OLIVEIRA M.C., *Comparison between Berkovich, Vickers and conical indentation tests: A three-dimensional numerical simulation study*, Int. J. Solids. Struct., 2009, 46, 1095–1104.

[21] SNEDDON I.N., *The relation between load and penetration in the axisymmetric Boussinesq a problem for a punch of arbitrary profiles*, Int. J. Eng. Sci., 1965, 3(1), 47–57.

[22] TOMANIK M., NICODEMUS A., FILIPIAK J., *Microhardness of human cancellous bone tissue in progressive hip osteoarthritis*, J. Mech. Behav. Biomed. Mater., 2016, 64, 86–93.

[23] VOYIADJIS G.Z., ALMASRI A.H., PARK T., *Experimental nanoindentation of BCC metals*, Mech. Res. Commun., 2010, 37(3), 307–314.

[24] WU Z., BAKER T.A., OVAERT T.C., NIEBUR G.L., *The effect of holding time on nanoindentation measurements of creep in bone*, J. Biomech., 2011, 44, 1066–1072.

[25] ZHAO M., OGASAWARA N., CHIBA N., CHEN X., *A new approach to measure the elastic-plastic properties of bulk materials using spherical indentation*, Acta Mater., 2006, 54, 23–32.